Desalination and Water Treatment
www.deswater.com

doi: 10.5004/dwt.2023.29785

303 (2023) 236–244
August

Efficient corn straw and poplar leaf biochar-based adsorbents for the eradication of methylene blue from aqueous solutions

Yue Zhao[a], Kezhen Qi[b,*], Jing Pan[a,*]

[a]*College of Life Science, Shenyang Normal University, Shenyang 110034, China, email: crystalpan@synu.edu.cn (J. Pan), ZhaoY_0234@163.com (Y. Zhao)*
[b]*College of Pharmacy, Dali University, Dali 671000, China, email: qkzh2003@aliyun.com (K. Qi)*

Received 2 April 2023; Accepted 16 July 2023

ABSTRACT

Using agricultural and forestry waste biomasses as raw materials for the removal of organic dyes from wastewater is a cost-effective approach for environmental purification. In this paper, corn straws and poplar leaves were carbonized at different temperatures for 3 h to produce biochar-based adsorbents. Afterwards, with the addition of the prepared adsorbents to methylene blue (MB) wastewater, the effects of contact time, initial concentration of MB and adsorbent dosage on the adsorption performance were investigated. Meanwhile, both adsorption kinetic models and adsorption isotherm models were also studied to explore adsorption mechanisms of the obtained adsorbents. The physico-chemical properties of biochar-based adsorbents were subsequently characterized by scanning electron microscopy and Brunauer–Emmett–Teller. The results demonstrated that two biochar-based adsorbents produced from corn straws and poplar leaves at 300°C after 3 h carbonization achieved the highest yields of 90.5% and 90.7%, respectively. The removal rate of MB increased with contact time and the adsorption capacity for MB enhanced with initial concentration of MB by biochar-based adsorbents prepared by corn straws and poplar leaves. The highest removal rate of MB was 99.2% for corn straws biochar-based adsorbent at a dosage of 1.0 g and 95.1% for poplar leaves biochar-based adsorbent at a dosage of 1.5 g. Furthermore, the adsorption process of MB by corn straw and poplar leaf biochar-based adsorbents conformed to the quasi-second-order adsorption kinetic model and Langmuir model, which was dominated by chemical adsorption.

Keywords: Agricultural and forestry biomasses; Slow pyrolysis method; Biochar; Methylene blue; Adsorption kinetics

1. Introduction

The rapid development of printing and dyeing processes has resulted in a large amount of printing and dyeing waste in waterbodies [1–4]. Methylene blue (MB) is a cationic alkaline dye with the chemical formula $C_{16}H_{18}ClN_3S$. Its extensive applications in industries such as chemistry, biology, as well as printing and dyeing have currently made it become a typical dye pollutant. MB may cause permanent damage to the eyes of humans and animals due to its characteristic of a certain degree of toxicity. It can cause symptoms such as nausea and diarrhoea by stimulating the gastrointestinal tract. It can also be inhaled into the respiratory tract through air medium, causing dyspnoea, nausea and vomiting. More seriously, large amounts of MB entering human bodies can lead to mental disorder and methemoglobinemia [5]. In addition, MB is prone to fading when exposed to light and water, and is difficult to be efficiently removed from aqueous solutions by commonly used decontamination techniques such as biological treatment and chemical precipitation [6]. Notably, removal of MB is extremely important to safeguard both aquatic and terrestrial lives.

* Corresponding author.

At present, various physical methods like filtration, ion exchange, osmosis and air stripping have been applied for treating organic dyes [7–11], but these simply transfer the pollutants to another phase instead [12–16]. The main shortcoming of the mentioned technologies is that they lack the broad scope of treatment efficiency required to reduce all types of organic dyes present in wastewater [17–20]. Adsorption is one of the primitive and cost-effective techniques to eradicate objectionable substances from aqueous environment [21–23]. Amongst different kinds of adsorbents, biochar-based adsorptive removal of hazardous materials is an attractive approach owing to the extremely rich physical properties of biochar. So far, it has been effectively utilized to absorb and remove heavy metal ions, dyes, phenols, and their derivatives as well as alleviate eutrophication of water [24–26]. Besides, a broad range of adsorptive materials have been tested for removal of organic dyes including activated carbon, silica, zeolite, sand, clay particles, etc. [27]. In particular, biochar made from solid wastes are applied in wastewater treatment of organic dyes prevalently [28,29]. Liu et al. [6] used corn straws as a raw material to produce biochar with slow pyrolysis, and then applied the obtained biochar to the improvement of MB wastewater after modified treatment by KOH and H_3PO_4. As a result, the maximum MB adsorption capacities of 230.39 and 1,406.43 mg/g were achieved by H_3PO_4 and KOH modification, respectively. Hoslett et al. [30] concluded that the adsorption of MB from aqueous solutions by biochar prepared from the pyrolysis of mixed municipal discarded material with 300°C carbonization for 12 h was in line with second-order kinetic model and Langmuir adsorption isotherm, which was monolayer adsorption.

In this study, corn straws and poplar leaves were selected for the preparation of extremely efficient and low-cost adsorbents at different carbonization temperatures (300°C, 400°C and 500°C), and various analytical techniques were subsequently adopted to figure out their morphologies through scanning electron microscopy (SEM) and Brunauer–Emmett–Teller (BET) measurements. The adsorptive efficiencies of the prepared adsorbents were investigated by studying the contact time, initial concentration of MB and dosage of them. Furthermore, both adsorption kinetic models and adsorption isotherm models were also established to clarify the adsorption process and mechanism.

2. Preparation and characterization

2.1. Biomass raw materials and chemicals

Corn straws were collected from farmland in Shenyang while poplar leaves were brought from an experimental field of Shenyang Normal University (Shenyang, China). Analytical grade MB and HCl were purchased from Shenyang Chemical Reagent Factory (Shenyang, China) while H_2SO_4 was purchased from Beijing Chemical Plant (Beijing, China).

2.2. Instruments

WG-220 electric blast drying oven, M/s: Tianjin Taist Instrument Co., Ltd., (Tianjin, China); 800 Y high-speed crusher, M/s: Yongkang Boou Hardware Products Co., Ltd. (Yongkang, China); KSW-6-12 electric furnace temperature control meter, M/s: Beijing Yongguangming Medical Instrument Factory (Beijing, China); GL124-1SCN electronic balance, M/s: Beijing Sartorius Scientific Instrument Co., Ltd., (Beijing, China); QYC-200 thermostatic oscillator, M/s: Shanghai Shengke Instrument Equipment Co., Ltd., (Shanghai, China); UV-5900 UV-visible spectrophotometer, M/s: Shanghai Yuanxian Instrument Co., Ltd., (Shanghai, China). The surface morphologies of corn straws and poplar leaves biochar-based adsorbents were analyzed by scanning electron microscopy (SEM, FEI Quanta FEG 450). The BET surface area and pore structure were studied by MicroActive ASAP 2460.

2.3. Preparation of biochar

First, corn straws and poplar leaves were separately cut into 1–2 cm segments, washed with deionized water five times, and dried in the open air. Then, with further drying in a drying cabinet at 105°C for 48 h, the dried materials were placed in a high-speed pulverizer for crushing. The pulverized powders were passed through a 100-mesh sieve and then carbonized at different temperatures (300°C, 400°C and 500°C) for 3 h in a covered crucible placed in a muffle furnace. After carbonization, the materials were cooled to room temperature, and rinsed with 18 MΩ ultrapure water until the filtrate became neutral. Finally, through oven drying, the materials were stored in plastic bags in a dessicator for further experimental procedures.

2.4. Morphology analysis

The surface morphologies of corn straws and poplar leaves biochar-based adsorbents were observed with SEM. The specific surface area and pore structure analysis was realized from the nitrogen physical adsorption–desorption isotherm of the biochar samples with the specific surface area and pore size analyzer at the liquid nitrogen bath temperature of 77.4 K. Meanwhile, the specific surface area and pore size of the biochar samples were calculated according to the BET multi-point method and Barrett–Joyner–Halenda theory.

2.5. Adsorption kinetic model

The experiments were carried out with 250 mL Erlenmeyer flasks containing 100 mL of MB solution at 35, 50, 80, and 100 mg/L concentration and 1.0 g of biochar. The samples were taken at different time points throughout the experiments (40–180 min). The amount of MB adsorbed onto biochar at time point t was calculated by the followings:

Quasi-first-order kinetic model: $$\ln\left(q_e - q_t\right) = -k_1 t + \ln q_e \quad (1)$$

Quasi-second-order kinetic model: $$\frac{t}{q_t} = \frac{1 + k_2 q_e t}{k_2 q_e^2} \quad (2)$$

where q_t refers to the capacity of biochar to adsorb MB at time point t, mg/g; q_e represents the adsorption amount of MB at equilibrium, mg/g; k_1 is the quasi-first-order adsorption

rate constant, min^{-1}; k_2 is the quasi-second-order adsorption rate constant, g/(mg·min); t means the adsorption time, min.

2.6. Adsorption isotherm model

Based on the above experimental parameters, a certain amount of biochar was added to a 50 mL conical flask containing different concentrations of MB solutions (35–100 mg/L). Then, the samples were placed in an oscillating oscillator operating at 180 rpm and maintained at 25°C for a period of time. The adsorption capacity of MB was subsequently measured by filtering the samples. The Langmuir model and Freundlich model were employed to fit the obtained adsorption thermodynamic data, with the following formulas:

$$\frac{1}{Q_e} = \frac{1}{q_m K_L C_e} + \frac{1}{q_m} \tag{3}$$

$$\ln Q_e = \ln K_F + \frac{1}{n} \ln C_e \tag{4}$$

where C_e and Q_e are MB concentration and adsorption capacity of biochar for MB at equilibrium, q_m stands for the maximum adsorption capacity of biochar for MB, mg/g; K_L denotes a parameter that characterizes the adsorption strength, mg/L; K_F is the Freundlich adsorption coefficient, $mg^{1-n}/g \cdot L^n$; n indicates the Freundlich constant.

2.7. Influence of contact time on adsorption

With the addition of 1.0 g biochar-based adsorbent to 100 mL MB solution with a concentration of 50 mg/L, the mixture was kept in a thermostatic oscillation water bath box at room temperature oscillating with a rate of 180 rpm. 1 mL of MB was separated after regular interval of time 40, 80, 120 and 180 min for measuring the concentration of MB to calculate the removal rate and adsorption amount at the given time.

2.8. Effect of initial concentration of MB on adsorption

With the addition of 1.0 g biochar-based adsorbent to 100 mL MB solutions with different concentrations (35, 50, 80 and 100 mg/L), the mixture was retained in a thermostatic oscillation water bath box at room temperature oscillating with a rate of 180 rpm. 1 mL of MB was separated after 120 min for measuring the concentration of MB to calculate the removal rate and adsorption amount at the given concentration.

2.9. Effect of biochar dosage on adsorption

With the addition of different weights of biochar adsorbents (0.5, 1.0 and 1.5 g) to 100 mL MB solution with a concentration of 50 mg/L, the mixture was kept in a thermostatic oscillation water bath box at 25°C oscillating with a rate of 180 rpm. 1 mL of MB was separated after 120 min for measuring the concentration of MB to calculate the removal rate and adsorption amount at the given concentration.

3. Results and discussion

3.1. Yield of biochar

Under the carbonization temperature of 300°C, the two adsorbents with corn straws and poplar leaves as raw materials were found to achieve the highest yields of 90.49% and 90.69%, respectively. With the increased temperature, the yields of tar and coke decreased slowly as chemical bonds and functional groups were fractured by long-term high temperature heating [31]. This further contributed to the easy decomposition of biomass and the increase of volatile components, causing the decreased yields of tar and coke [32]. Thus, corn straws and poplar leaves were regarded as good raw materials for preparing biochar-based adsorbents, with carbonization of biochar at 300°C for 3 h as the optimal conditions.

3.2. Morphology of the adsorbents

It can be seen from Fig. 1 that the adsorbents prepared from corn straws and poplar leaves biochar at 300°C were lamellar of 1 μm size. Obvious irregular granular pores and relatively complex porous structure were observed at 5 μm, which was due to the decomposition of biomass during carbonization [33]. Through comparison, it was found that granular pores of corn straws biochar were more obvious, providing large surface area for the adsorption of more MB particles, which was also consistent with the result that the adsorption effect of corn straws biochar-based adsorbent was better than that of poplar leaves biochar-based adsorbent.

3.3. BET analysis

To further study the porous structure of the samples, N_2 adsorption and desorption tests were carried out for each sample as shown in Table 1 and Fig. 2. From BET measurement, it was found that the specific surface area of corn straws biochar was smaller than that of poplar leaves, but the pore volume and pore size of corn straws biochar were significantly larger than that of poplar leaves biochar, which was in good agreement with the results of SEM. It is generally accepted that the pore size greater than 50 nm (64.1 nm) is called macropore and the pore size less than 50 nm (23.7 nm) is called mesoporous. Therefore, corn straws biochar was mainly macropore, while poplar leaves biochar was primarily mesoporous. The research demonstrated that the macropore of corn straws biochar matched the particle size of the MB molecular aggregate, thus exhibiting high adsorption ability.

3.4. Influence of contact time on adsorption process

Fig. 3 shows that adsorption of MB on all experimental materials increased with contact time. Soni et al. drew the same conclusion in his research of using cobalt doped iron-based metal–organic frameworks (MOF) for enhanced removal and recovery of MB from wastewater [34]. The removal rate and adsorption capacity of MB by corn straws and poplar leaves were lower than those of their biochar products. Interestingly, the adsorption ability of corn straws

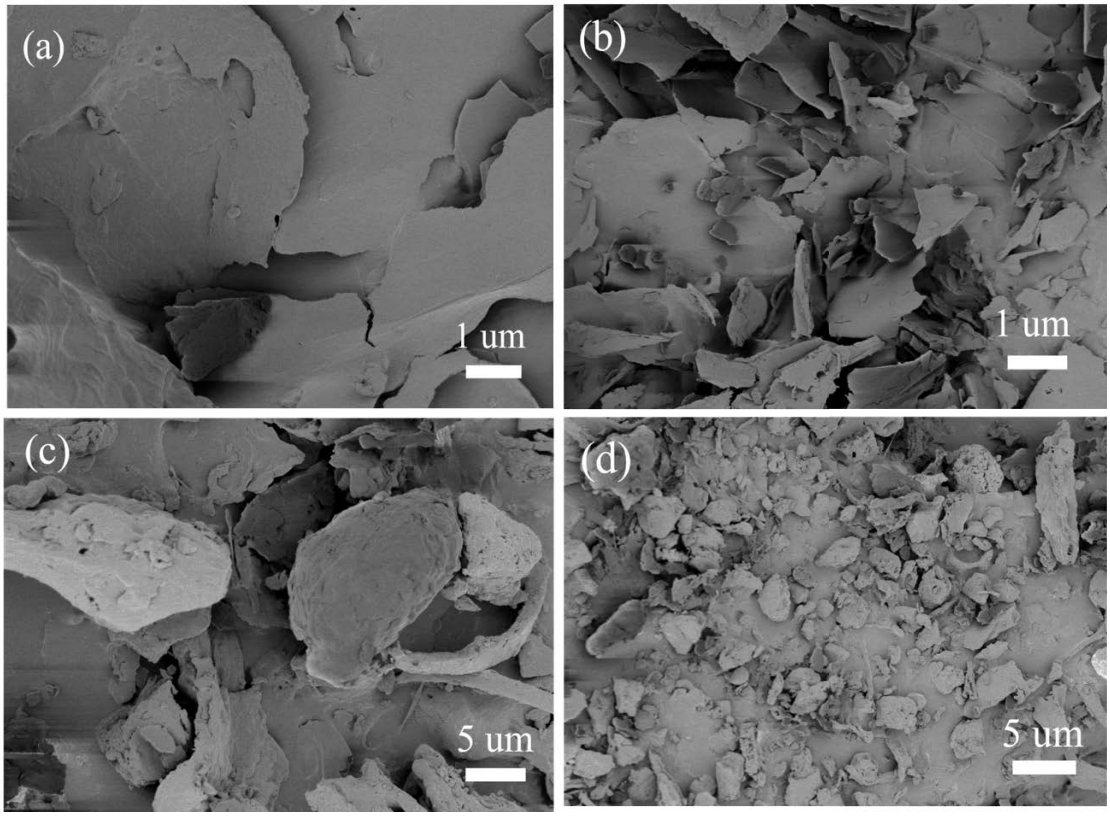

Fig. 1. Scanning electron microscopy images of corn straws biochar (a,c) and poplar leaves biochar (b,d) produced at 300°C.

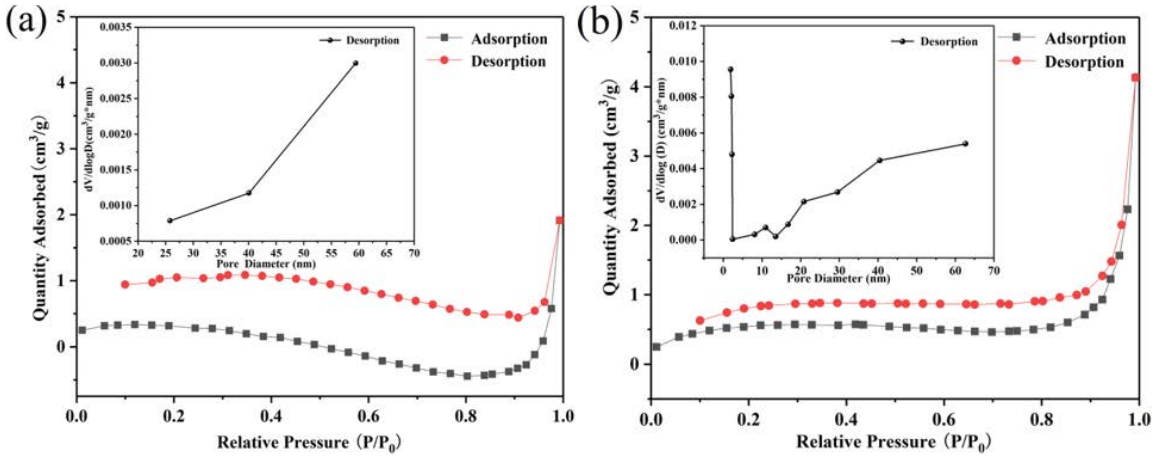

Fig. 2. Adsorption–desorption curve and pore-size distribution of corn straws (a) and poplar leaves (b) biochar.

Table 1
Surface area, pore volume and pore size of biochar produced from corn straws and poplar leaves

Sample	Surface area (m^2/g)	Pore volume (cm^3/g)	Pore size (nm)
Corn straws	0.863	7.88×10^{-4}	64.1
Poplar leaves	1.76	1.93×10^{-4}	23.7

biochar-based adsorbent prepared at 400°C for MB was the highest, with 3.31 mg/g MB removed along with a removal rate of 99.30%. However, the adsorbent obtained from poplar leaves biochar heated at 500°C realized an adsorption of 3.20 mg/g MB with a removal rate of 96.09%. Obviously, under the same preparation conditions, the adsorption performance of corn straws biochar was superior to that of poplar leaves biochar. Further, adsorbents prepared at higher carbonization temperature were proved to be more

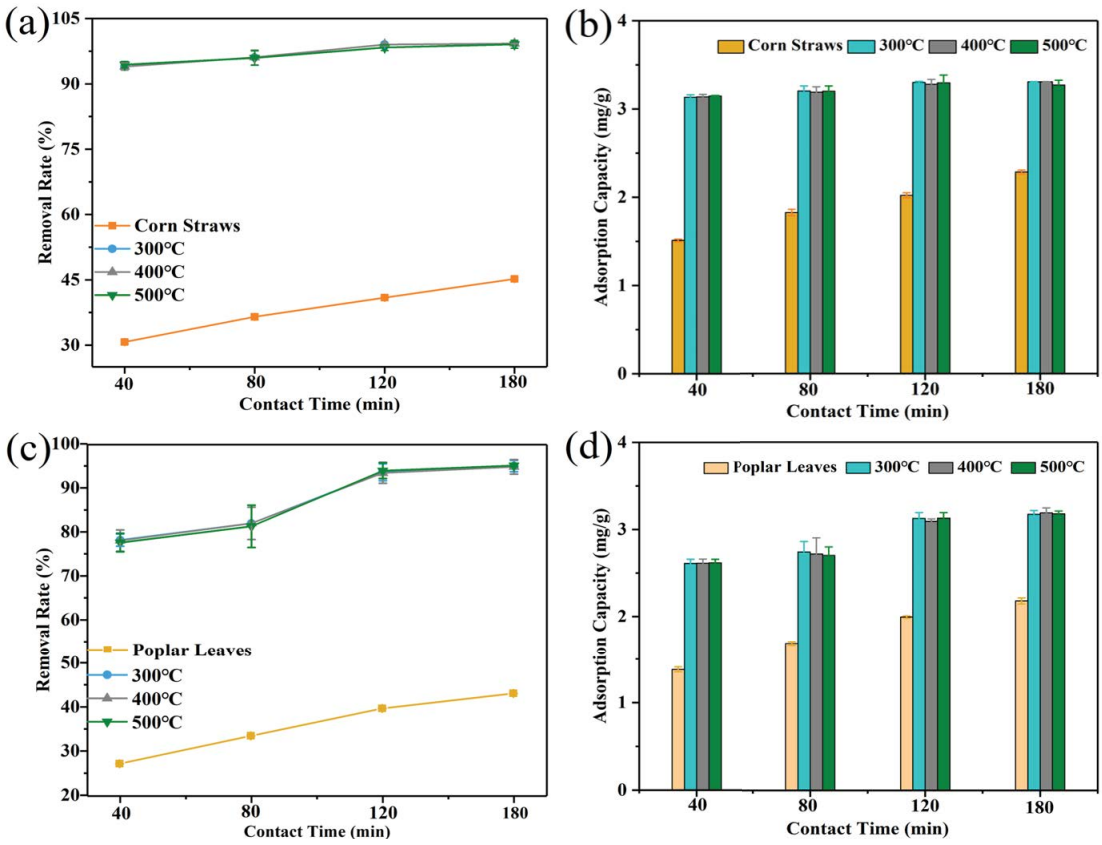

Fig. 3. Removal rate and adsorption capacity of methylene blue by corn straws biochar (a,b) and poplar leaves (c,d) biochar at different time points.

active than those prepared at lower temperature [35]. With the extension of contact time, the pores of biochar-based adsorbents were occupied by MB particles, leading to the saturated surfaces of the adsorbents. At this stage, with the maximum adsorption capacity reached, a dynamic equilibrium was established between the adsorbed MB particles and particles of MB in the solution.

3.5. Effect of initial concentration of MB

It was obvious from Fig. 4 that when the initial concentration of MB was increased from 35 to 100 mg/L, adsorption of MB onto the surface of the adsorbents increased remarkably. The adsorption capacity of biochar heated at 400°C for 3 h reached the highest at 100 mg/L of MB concentration. The adsorbent prepared from corn straws removed about 6.25 mg/g MB while the adsorbent prepared from poplar leaves eradicated 5.30 mg/g MB. Clearly, the effect of concentration on the adsorption performance was more significant than contact time. When the concentration of MB was apparently increased, the rate of diffusion of MB particles increased, resulting in more pronounced adsorption effect.

3.6. Influence of the amount of biochar on adsorption

From Fig. 5 it is observed that as the amount of biochar increased from 0.5 to 1.5 g, the removal rate of MB displayed a significant upward trend, while the adsorption amount presented an opposite trend. This was because the surface adsorption sites also increased with the increased amount of carbon. However, under a certain level of concentration, the adsorption sites gradually saturated with the increase of carbon used, leading to the decreased adsorption capacity per unit of biochar. Therefore, the removal rate and adsorption capacity trends were completely opposite. The adsorption capacity reached the highest at the dosage of 0.5 g biochar. Under these conditions, corn straws biochar-based adsorbent removed approximately 9.51 mg/g MB, while poplar leaves biochar-based adsorbent eliminated approximately 8.12 mg/g MB. Moreover, the highest MB removal rates of corn straws and poplar leaves biochar-based adsorbents were 99.2% at a dosage of 1.0 g and 95.1% at a dosage of 1.5 g, respectively.

3.7. Adsorption kinetic model

To further explore the adsorption process, kinetic curves for the adsorption of MB by biochar-based adsorbents were fitted with first and second-order models. The fitting results are summarized in Table 2 and Fig. 6. It could be seen that the adsorption rate of corn straws biochar-based adsorbent was higher than that of poplar leaves biochar-based adsorbent. The adsorption process of MB by corn straws and poplar leaves biochar-based adsorbents conformed to

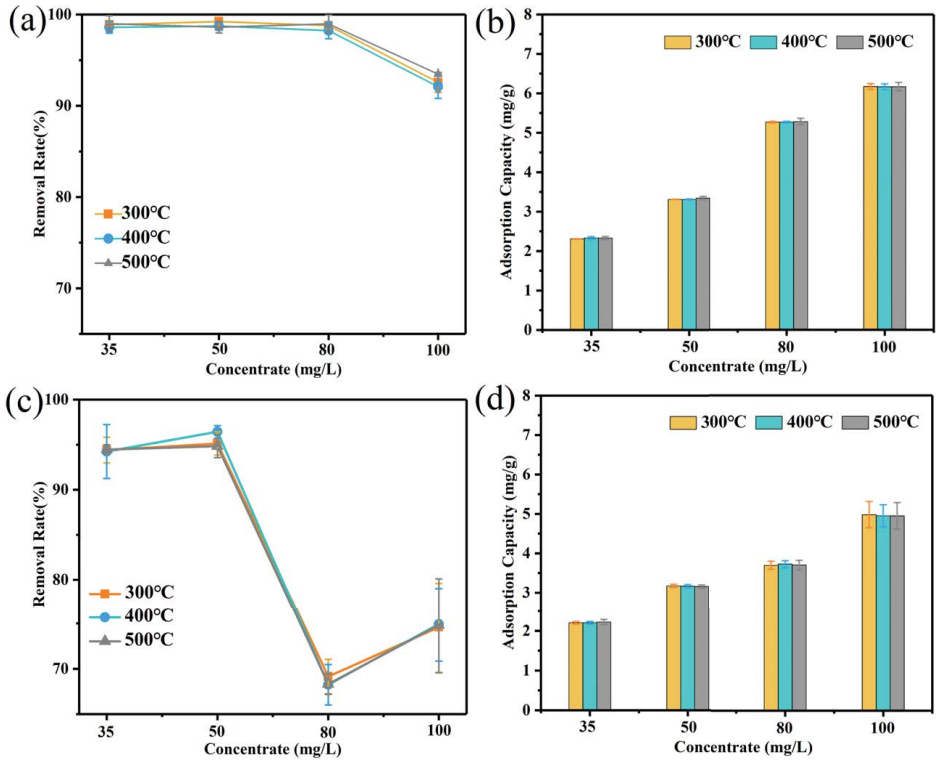

Fig. 4. Removal rate and adsorption capacity of methylene blue by corn straws biochar (a,b) and poplar leaves (c,d) biochar at different concentrations.

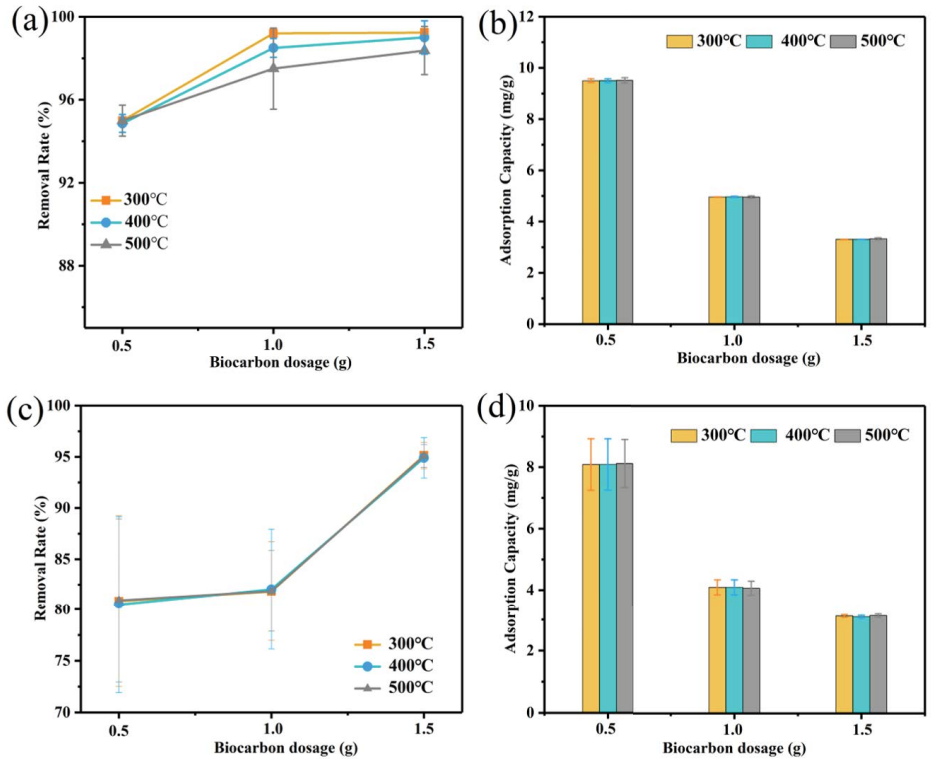

Fig. 5. Removal rate and adsorption capacity of methylene blue by corn straws biochar (a,b) and poplar leaves (c,d) biochar with different dosages.

Table 2
Adsorption kinetic parameters of methylene blue by biochar produced from corn straws and poplar leaves

Types of biochar	Quasi-first-order kinetic model			Quasi-second-order kinetic model		
	k_1 (min^{-1})	q_e (mg/g)	R^2	k_2 (g/mg·min)	q_e (mg/g)	R^2
Corn straws	4.35×10^{-2}	3.31	0.975	1.60×10^{-3}	3.31	0.999
Poplar leaves	2.12×10^{-2}	3.20	0.963	5.01×10^{-4}	3.20	0.999

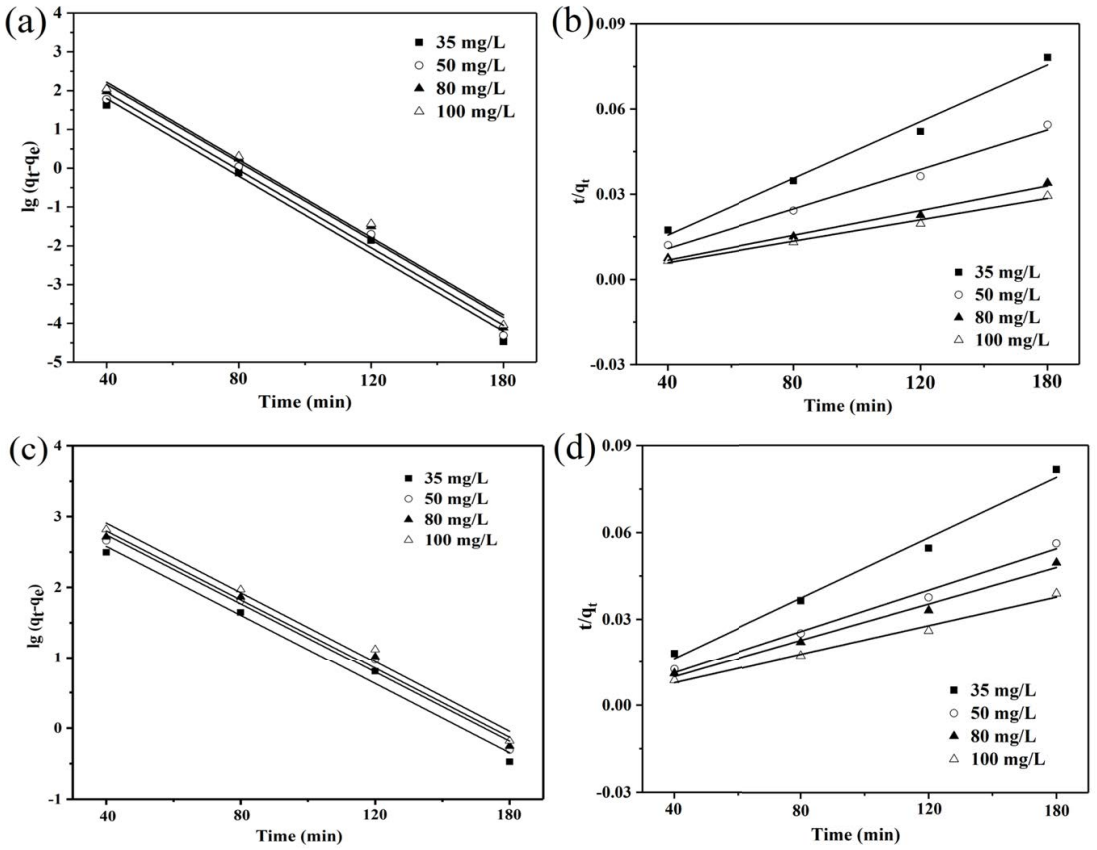

Fig. 6. Kinetic model of methylene blue adsorption on corn straws biochar (a,b) and poplar leaves (c,d) biochar.

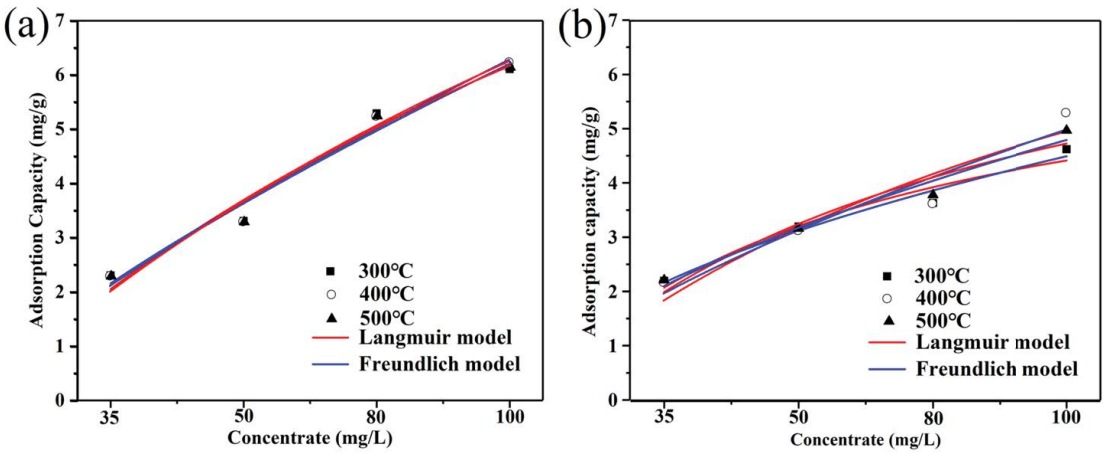

Fig. 7. Isotherm model of methylene blue adsorption on corn straws biochar (a) and poplar leaves (b) biochar.

Table 3
Isothermal parameters of methylene blue adsorption on biochar prepared from corn straws and poplar leaves

Types of biochar	Freundlich model			Langmuir model		
	K_F (mg/g)(L/mg)$^{1/n}$	$1/n$	R^2	q_m (mg/g)	K_L (mg/L)	R^2
Corn straw	0.226	0.685	0.973	6.25	0.895	0.997
Poplar leaves	0.100	0.887	0.953	5.30	0.762	0.991

the quasi-second-order adsorption kinetic model with R^2 value of 0.999, which belonged to chemical adsorption of the single molecular layer. The results were consistent with the research findings of iron-based metal organic framework for efficient removal of MB from industrial waste by Arora et al. [36]. However, chemical adsorption of the single molecular layer occupied a dominating position during the process of removing MB from aqueous solution by sewage sludge-derived biochar [37]. In addition, the transfer of common electron pairs between the MB molecule and biochar occurred [38] resulted in the degradation of MB due to the role of chemical bonds [39].

3.8. Adsorption isotherm model

As can be seen from Fig. 7 and Table 3, the adsorption processes of MB by corn straws and poplar leaves biochar were more closely fitted to the Langmuir model with R^2 between 0.991 and 0.997. According to the Q_m value, it was suggested that corn straws were more suitable as a raw material for biochar. The value of $1/n$ less than 1 indicated that the adsorption processes of MB by the two types of biochar were relatively easy to occur. Besides, the maximum adsorption capacities of corn straws biochar and poplar leaves biochar were 6.25 and 5.30 mg/g, respectively, which were 2.75 and 2.47 times that of corn straws (Q_m = 2.27 mg/g) and poplar leaves (Q_m = 2.15 mg/g).

4. Conclusion

Corn straws and poplar leaves were proved to be excellent raw materials for the preparation of biochar-based adsorbents to remove MB from aqueous solutions. The highest yields of corn straw and poplar leaf biochar-based adsorbents were 90.5% and 90.7% produced at 300°C for 3 h, respectively. The highest MB removal rates of corn straw and poplar leaf biochar-based adsorbents were 99.2% at a dosage of 1.0 g, and 95.1% at a dosage of 1.5 g, respectively. It was confirmed that contact time and initial concentration of MB affected the removal rate and the adsorption capacity of the two types of prepared adsorbents for MB. Apart from that, the adsorption processes of MB by corn straw and poplar leaf biochar-based adsorbents corresponded to the quasi-second-order adsorption kinetic model and the Langmuir model.

Acknowledgments

This work was financially supported by Applied Basic Research Plan of Liaoning (2023JH2/101300053), Science and Technology Plan of Shenyang (21-108-9-36), Major Original Program in Shenyang Normal University (ZD201904), the Ninth Batch of Education and Teaching Reform Project of Shenyang Normal University (JG2021-YB099), NSFC (22268003, 52272287, 22202138), Project from Yunnan Province (202301AT070027, 202305AF150116) and Dali University (KY2296129740).

References

[1] K. Qi, S. Karthikeyan, W. Kim, F.A. Marzouqi, I.S. Al-Khusaibi, Y. Kim, R. Selvaraj, Hydrothermal synthesis of SnS_2 nanocrystals for photocatalytic degradation of 2,4,6-trichlorophenol under white LED light irradiation, Desal. Water Treat., 92 (2017) 108–115.
[2] G. Enaime, A. Baçaoui, A. Yaacoubi, M. Lübken, Biochar for wastewater treatment—conversion technologies and applications, Appl. Sci. Basel., 10 (2020) 492, doi: 10.3390/app10103492.
[3] C. Arora, P. Kumar, S. Soni, J. Mittal, A. Mittal, B. Singh, Efficient removal of malachite green dye from aqueous solution using *Curcuma caesia* based activated carbon, Desal. Water Treat., 195 (2020) 341–352.
[4] K. Qi, S. Liu, Q. Meng, Photocatalytic performance of TiO_2 nanocrystals with/without oxygen defects, Chin. J. Catal., 39 (2018) 867–875.
[5] P.O. Oladoye, T.O. Ajiboye, E.O. Omotola, O.J. Oyewola, Methylene blue dye: toxicity and potential elimination technology from wastewater, Results Eng., 16 (2022) 100678, doi: 10.1016/j.rineng.2022.100678.
[6] L. Liu, Y. Li, S.S. Fan, Preparation of KOH and H_3PO_4 modified biochar and its application in methylene blue removal from aqueous solution, Processes, 7 (2019) 891, doi: 10.3390/pr7120891.
[7] J. Mittal, R. Ahmad, A. Mittal, Kahwa tea (*Camellia sinensis*) carbon — a novel and green low-cost adsorbent for the sequestration of titan yellow dye from its aqueous solutions, Desal. Water Treat., 227 (2021) 404–411.
[8] H. Daraei, A. Mittal, Investigation of adsorption performance of activated carbon prepared from waste tire for the removal of methylene blue dye from wastewater, Desal. Water Treat., 90 (2017) 294–298.
[9] K. Zhang, J. Zhang, X. He, Y. Zhao, A. Zada, A. Peng, K. Qi, Fe_3O_4@MIL-100(Fe) modified ZnS nanoparticles with enhanced sonocatalytic degradation of tetracycline antibiotic in water, Ultrason. Sonochem., 95 (2023) 106409, doi: 10.1016/j.ultsonch.2023.106409.
[10] Y. Ma, X. Aihemaiti, K. Qi, S. Wang, Y. Shi, Z. Wang, M. Gao, F. Gai, Y. Qiu, Construction of oxygen-vacancies-rich S-scheme $BaTiO_3$/red phosphorous heterojunction for enhanced photocatalytic activity, J. Mater. Sci. Technol., 156 (2023) 217–229.
[11] R. Kayisier, Y. Ma, K. Qi, L. Xiao, Y. Wang, Y. Li, J. Li, Y. Li, Synergetic removal of mixed pollutants over cerium oxide/red phosphorus heterojunction composite, Vacuum, 213 (2023) 112068, doi: 10.1016/j.vacuum.2023.112068.
[12] P. Wony, M. Runowski, S. Sobczak, A. Szczeszak, S.J.C.I. Lis, Corrigendum to high-pressure luminescence of monoclinic and triclinic $GdBO_3$: Eu^{3+}, Ceram. Int., 46 (2020) 26368–26376.
[13] K. Qi, C. Zhuang, M. Zhang, P. Gholami, A. Khataee, Sonochemical synthesis of photocatalysts and their applications, J. Mater. Sci. Technol., 123 (2022) 243–256.

[14] J. Zhang, A. Bifulco, P. Amato, C. Imparato, K. Qi, Copper indium sulfide quantum dots in photocatalysis, J. Colloid Interface Sci., 638 (2023) 193–219.
[15] K. Qi, X. Xing, A. Zada, M. Li, Q. Wang, S.-y. Liu, H. Lin, G. Wang, Transition metal doped ZnO nanoparticles with enhanced photocatalytic and antibacterial performances: experimental and DFT studies, Ceram. Int., 46 (2020) 1494–1502.
[16] N. Cui, A. Zada, J. Song, Y. Yang, M. Liu, Y. Wang, Y. Wu, K. Qi, R. Selvaraj, S.-y. Liu, G. Jin, Plasmon-induced ZnO-Ag/AgCl photocatalyst for degradation of tetracycline hydrochloride, Desal. Water Treat., 245 (2022) 247–257.
[17] J. Zhang, Y. Zhao, K. Zhang, A. Zada, K. Qi, Sonocatalytic degradation of tetracycline hydrochloride with $CoFe_2O_4$/g-C_3N_4 composite, Ultrason. Sonochem., 94 (2023) 106325, doi: 10.1016/j.ultsonch.2023.106325.
[18] L. Sun, Y. Wang, L. He, J. Guo, Q. Deng, X. Zhao, Y. Yan, K. Qi, Effect of cobalt doping on the photocatalytic performance of $AgInS_2$ for organic pollutant degradation and hydrogen production, J. Alloys Compd., 926 (2022) 166859, doi: 10.1016/j.jallcom.2022.166859.
[19] K. Qi, S. Liu, R. Wang, Z. Chen, R. Selvaraj, P_t/g-C_3N_4 composites for photocatalytic H_2 production and $^{\bullet}OH$ formation, Desal. Water Treat., 154 (2019) 312–319.
[20] K. Qi, S.-y. Liu, R. Selvaraj, W. Wang, Z. Yan, Comparison of P_t and Ag as co-catalyst on g-C_3N_4 for improving photocatalytic activity: experimental and DFT studies, Desal. Water Treat., 153 (2019) 244–252.
[21] A. Patel, S. Soni, J. Mittal, A. Mittal, C. Arora, Sequestration of crystal violet from aqueous solution using ash of black turmeric rhizome, Desal. Water Treat., 220 (2021) 342–352.
[22] J. Mittal, R. Ahmad, M.O. Ejaz, A. Mariyam, A. Mittal, A novel, eco-friendly bio-nanocomposite (Alg-Cst/Kal) for the adsorptive removal of crystal violet dye from its aqueous solutions, Int. J. Phytorem., 24 (2022) 796–807.
[23] A. Mariyam, J. Mittal, F. Sakina, R.T. Baker, A.K. Sharma, A. Mittal, Efficient batch and fixed-bed sequestration of a basic dye using a novel variant of ordered mesoporous carbon as adsorbent, Arabian J. Chem., 14 (2021) 103186, doi: 10.1016/j.arabjc.2021.103186.
[24] X. He, J. Xia, J. He, K. Qi, A. Peng, Y. Liu, Highly efficient capture of heavy metal ions on amine-functionalized porous polymer gels, Gels, 9 (2023) 297, doi: 10.3390/gels9040297.
[25] R. Ahmad, I. Hasan, A. Mittal, Adsorption of Cr(VI) and Cd(II) on chitosan grafted polyaniline-OMMT nanocomposite: isotherms, kinetics and thermodynamics studies, Desal. Water Treat., 58 (2017) 144–153.
[26] J. Mittal, R. Ahmad, A. Mariyam, V.K. Gupta, A. Mittal, Expeditious and enhanced sequestration of heavy metal ions from aqueous environment by papaya peel carbon: a green and low-cost adsorbent, Desal. Water Treat., 210 (2021) 365–376.
[27] V. Kumar, P. Saharan, A.K. Sharma, A. Umar, I. Kaushal, A. Mittal, Y. Al-Hadeethi, B. Rashad, Silver doped manganese oxide-carbon nanotube nanocomposite for enhanced dye-sequestration: isotherm studies and RSM modelling approach, Ceram. Int., 46 (2020) 10309–10319.
[28] C.T. Nguyen, D. Tungtakanpoung, V.T. Tra, P. Kajitvichyanukul, Kinetic, isotherm and mechanism in paraquat removal by adsorption process using corn cob biochar produced from different pyrolysis conditions, Case Stud. Chem. Environ. Eng., 6 (2022) 100248, doi: 10.1016/j.cscee.2022.100248.
[29] Y. Zhang, S. Fan, T. Liu, W. Fu, B. Li, A review of biochar prepared by microwave-assisted pyrolysis of organic wastes, Sustainable Energy Technol. Assess., 50 (2022) 101873, doi: 10.1016/j.seta.2021.101873.
[30] J. Hoslett, H. Ghazal, N. Mohamad, H. Jouhara, Removal of methylene blue from aqueous solutions by biochar prepared from the pyrolysis of mixed municipal discarded material, Sci. Total Environ., 714 (2020) 136832, doi: 10.1016/j.scitotenv.2020.136832.
[31] K. Weber, P. Quicker, Properties of biochar, Fuel, 217 (2018) 240–261.
[32] Z. Jin, B. Wang, L. Ma, P. Fu, L. Xie, X. Jiang, W. Jiang, Air pre-oxidation induced high yield N-doped porous biochar for improving toluene adsorption, Chem. Eng. J., 385 (2020) 123843, doi: 10.1016/j.cej.2019.123843.
[33] P. Zhang, D. O'Connor, Y. Wang, L. Jiang, T. Xia, L. Wang, D.C.W. Tsang, Y.S. Ok, D. Hou, A green biochar/iron oxide composite for methylene blue removal, J. Hazard. Mater., 384 (2020) 121286, doi: 10.1016/j.jhazmat.2019.121286.
[34] S. Soni, P.K. Bajpai, J. Mittal, C. Arora, Utilisation of cobalt doped iron-based MOF for enhanced removal and recovery of methylene blue dye from wastewater, J. Mol. Liq., 314 (2020) 113642, doi: 10.1016/j.molliq.2020.113642.
[35] I. Khalaf Erabee, Removal of ammonia nitrogen NH-N and hexavalent chromium (VI) from wastewater using agricultural waste activated carbon, Orient. J. Chem., 34 (2018) 1033–1040.
[36] C. Arora, S. Soni, S. Sahu, J. Mittal, P. Kumar, P.K. Bajpai, Iron based metal organic framework for efficient removal of methylene blue dye from industrial waste, J. Mol. Liq., 284 (2019) 343–352.
[37] S. Fan, Y. Wang, Z. Wang, J. Tang, J. Tang, X. Li, Removal of methylene blue from aqueous solution by sewage sludge-derived biochar: adsorption kinetics, equilibrium, thermodynamics and mechanism, J. Environ. Chem. Eng., 5 (2017) 601–611.
[38] H. Chen, W. Li, J. Wang, H. Xu, Y. Liu, Z. Zhang, Y. Li, Y. Zhang, Adsorption of cadmium and lead ions by phosphoric acid-modified biochar generated from chicken feather: selective adsorption and influence of dissolved organic matter, Bioresour. Technol., 292 (2019) 121948, doi: 10.1016/j.biortech.2019.121948.
[39] Q. Huang, S. Song, Z. Chen, B. Hu, J. Chen, X. Wang, Biochar-based materials and their applications in removal of organic contaminants from wastewater: state-of-the-art review, Bioresour. Technol., 1 (2019) 45–73.